

Clinical Paper  
Reconstructive Surgery

# Accurate occlusion-driven maxillary reconstruction with deep circumflex iliac artery flap using computer-assisted techniques and intraoral anastomosis: a case series

S.-Y. Qiu<sup>1</sup>, X.-F. Shan<sup>1</sup>, Y.-F. Kang,  
M.-K. Ding, L. Zhang, Z.-G. Cai

Department of Oral and Maxillofacial Surgery, Peking University School and Hospital of Stomatology, Haidian District, Beijing, China

S.-Y. Qiu, X.-F. Shan, Y.-F. Kang, M.-K. Ding, L. Zhang, Z.-G. Cai: *Accurate occlusion-driven maxillary reconstruction with deep circumflex iliac artery flap using computer-assisted techniques and intraoral anastomosis: a case series. Int. J. Oral Maxillofac. Surg. 2023; 52: 744–752.* © 2022 Published by Elsevier Inc. on behalf of International Association of Oral and Maxillofacial Surgeons.

**Abstract.** The aim of this study was to evaluate the feasibility and accuracy of occlusion-driven maxillary reconstruction with the deep circumflex iliac artery (DCIA) flap, using computer-assisted design and manufacturing (CAD/CAM) technology and intraoral anastomosis. The data of 11 patients who underwent occlusion-driven maxillary reconstruction with this method between December 2018 and December 2020 in the Department of Oral and Maxillofacial Surgery, Peking University School and Hospital of Stomatology were reviewed retrospectively. Postoperative complications and functional and aesthetic outcomes were recorded. The accuracy of the postoperative restoration was assessed using Geomagic Control 2014. Reconstruction was successful in nine patients; all were satisfied with their aesthetic and functional outcomes. One patient underwent extraoral anastomosis after failure of intraoral anastomosis. In another patient, the DCIA flap had to be removed after the operation because of flap failure. Among the 10 patients with DCIA flap success, colour map analysis showed a mean deviation of  $0.40 \pm 0.08$  mm between the preoperative and postoperative craniomaxillary models. Thus, occlusion-driven maxillary reconstruction with the DCIA flap, using CAD/CAM technology and intraoral anastomosis, appears to be a feasible and accurate method for the repair of maxillary defects.

**Keywords:** Maxilla; Reconstructive surgical procedures; Free tissue flaps; Dental occlusion; Surgical anastomosis; Computer-aided design.

Accepted for publication 20 October 2022  
Available online 14 November 2022

<sup>1</sup> Shi-Yu Qiu and Xiao-Feng Shan are co-first authors.

Maxillary reconstruction is a challenging procedure in oral and maxillofacial surgery, because of the complex morphology of the region and the crucial importance of restoring function and appearance.<sup>1,2</sup> With the development of microsurgical techniques over the past three decades, a variety of free vascularized flaps have been applied for maxillary reconstruction.<sup>3</sup> Among these, the deep circumflex iliac artery (DCIA) flap is especially suitable for maxillary reconstruction,<sup>4</sup> although the short vascular pedicle and the difficult harvesting are major shortcomings.<sup>5,6</sup> The development of computer-assisted design/computer-assisted manufacturing (CAD/CAM) technology and intraoral anastomosis techniques has provided new ways to surmount the limitations of the DCIA flap. The aim of this study was to describe occlusion-driven maxillary reconstruction with the DCIA flap using CAD/CAM technology and intraoral anastomosis, and to evaluate its feasibility, accuracy, and advantages.

## Materials and methods

Between December 2018 and December 2020, a total of 11 patients underwent occlusion-driven maxillary reconstruction with the combination of CAD/CAM and intraoral anastomosis techniques at Peking University School and Hospital of Stomatology. Patients were considered eligible for this method of reconstruction if (1) they had a maxillary defect ranging in size from 2 cm to 8 cm, and (2) they had been diagnosed with a benign lesion or tumour and low-grade malignancy. The clinical and follow-up data of these patients were retrieved from the hospital records and reviewed retrospectively.

The study was approved by the Ethics Committee of Peking University School of Stomatology (approval number PKUSSIRB202055065).

### Virtual surgical planning and creation of the pre-bent titanium plate

The first step was the design of the tumour resection. Virtual surgical planning was performed by a team comprising oral and maxillofacial surgeons and prosthodontists. Before tumour resection, spiral computed tomography (CT) scans of the maxillofacial and iliac regions were performed (helix with 1.25-mm slice thickness; BrightSpeed 16-slice CT scanner; GE Healthcare, Buckinghamshire, UK) and the data were stored in DICOM format (Digital Imaging and Communication in

Medicine). ProPlan CMF 3.0 (Materialise, Leuven, Belgium) was used for three-dimensional (3D) reconstruction of the skull. The mandible was removed from the reconstructed skull to obtain the craniomaxillary model. The tumour outline was traced layer by layer, and the osteotomy planes were designed accordingly. The virtual resection was executed, and the craniomaxillary model with the expected postoperative defect was obtained. The distance between the osteotomy plane and the tumour boundary was at least 0.5 cm for benign tumours and 1 cm for malignant tumours (Fig. 1A).

The second step was the design of the maxillary reconstruction. The final occlusion was taken into consideration from the beginning of the maxillary reconstruction plan. The process was as follows: the dentition and occlusion in the defect area were restored virtually using a mirror technique (Fig. 1B). Afterwards, iliac block was placed in the defect area according to the restored dentition. The iliac crest should be placed along the alveolar bone restored virtually in the first step. Thus, an appropriate intermaxillary distance and suitable sites for implant positions could be achieved. Next, keeping the iliac crest still, the iliac block was rotated to restore the maxillary buttress. By doing so, the iliac block could provide mechanical support for subsequent implants and denture. Finally, a corresponding DCIA flap was cut, and virtual reconstruction of the maxilla was performed (Fig. 1C, D).

The third step was consideration of the subsequent intraoral anastomosis. Enough space was provided for the vascular pedicle of the DCIA flap. First, on the medial side of the iliac block, part of the hard palate was resected, even if not affected by the tumour, in order to prevent the medial vessels from being compressed (Fig. 2A). Second, if the pterygoid process and part of the posterior maxilla were preserved, a passage needed to be created at the posterior border of the defect area, through which the flap vessels could pass in order to reach the recipient vessels on the buccal mucosa (Fig. 2B).

The fourth step was the creation of the pre-bent titanium plate. The reconstructed craniomaxillary model was exported in STL format (stereolithography) (Fig. 1C), and a 3D model was printed using photosensitive resin material. The titanium plate (Johnson & Johnson, New Brunswick, NJ, USA) was bent to fit the model (Fig. 1D).

## Surgical procedure

Step 1 of the surgical procedure was tumour resection guided by a computer-assisted navigation system. The VectorVision navigation system was used (Brainlab, Munich, Germany). After the tumour had been resected, the navigation system was used again to verify the defect area. The VectorVision navigation system is a widely used computer-assisted intraoperative real-time navigation system. The feasibility and accuracy of the VectorVision navigation system has been well established.<sup>7-9</sup>

Step 2 was exposure and preparation of the recipient vessels. For the intraoral anastomosis, the patient was positioned supine, with the head turned 90° to the recipient side. A tongue retractor and deep retractor were used to fully expose the buccal mucosa of the recipient area. An oblique incision was made anterior to the Stensen duct, and the buccinator muscle was dissected to expose the buccal fat pad. The facial vessels were exposed by blunt dissection to avoid injury. A retrograde dissection was then performed to obtain an adequate pedicle length (usually 4 cm) and vessel calibre for subsequent intraoral microvascular anastomosis. Care was taken to identify and protect the mandibular branch of the facial nerve, which usually runs near the facial vessels.

Step 3 was harvesting of the DCIA flap using an individualized surgical guide. The individualized 3D-printed iliac osteotomy guides were designed using CAD software. The surgical area was routinely exposed through an incision above the anterior superior iliac spine along the iliac crest. The length of the incision depended on the required length of harvested iliac block. The DCIA and deep circumflex iliac vein were dissected and carefully protected for subsequent microvascular anastomosis. The 3D-printed iliac osteotomy guide was placed on the lateral aspect of the iliac crest and fixed with titanium screws, and the required iliac block was cut and shaped (Fig. 3A, B).

Step 4 was the placement and fixation of the DCIA flap. The pre-bent titanium plate was placed on the remnant maxilla and fixed with titanium screws. Then, the shaped DCIA flap was positioned in the defect area and fixed to the pre-bent titanium plate with titanium screws (Fig. 4A). After correct positioning of the flap had been confirmed by the VectorVision navigation system, the flap was removed to allow the intraoral anastomosis to be performed. It was then replaced and fixed to the pre-bent titanium plate again.

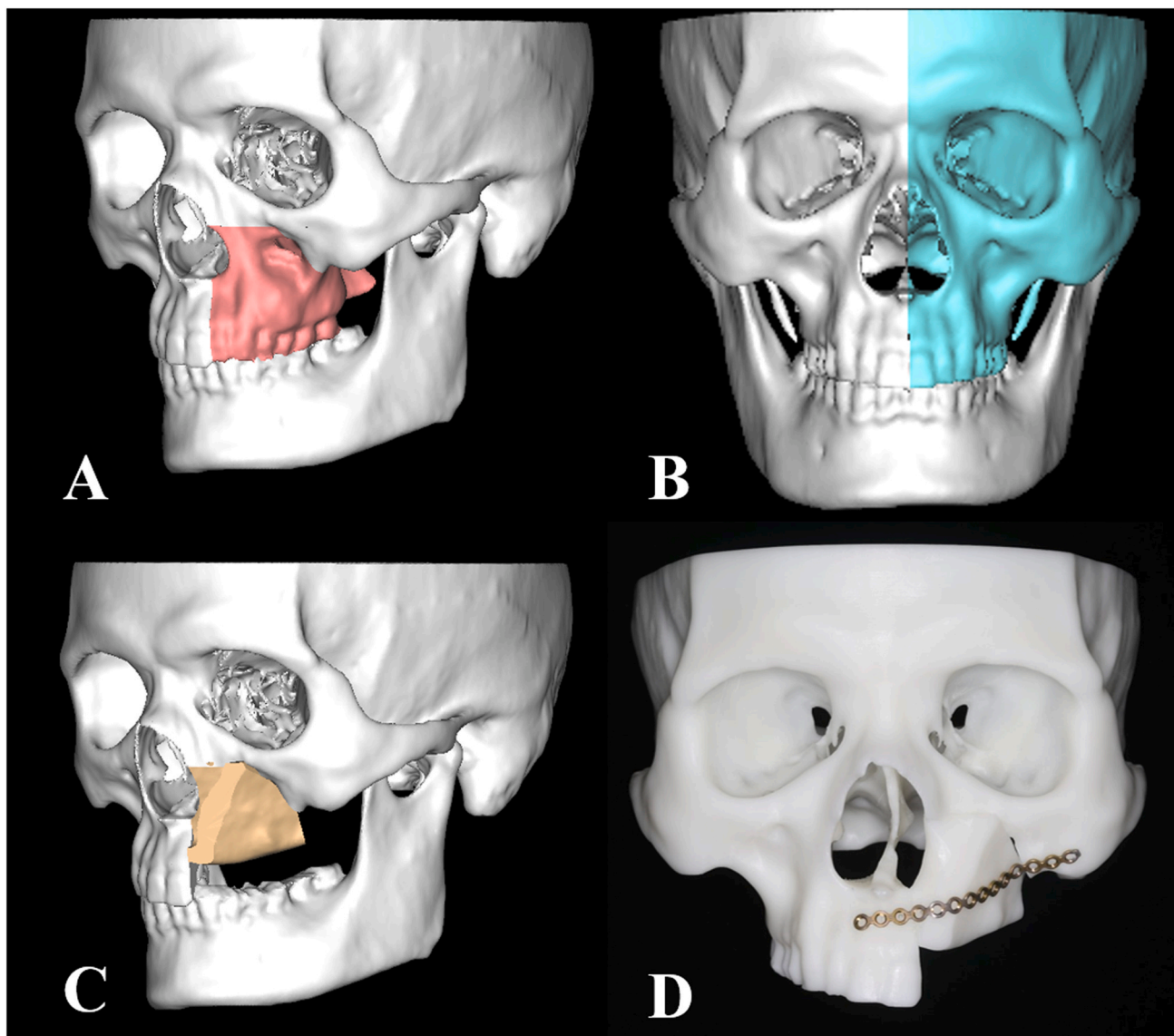


Fig. 1. Preoperative design process: (A) tumour resection design; (B) mirror technique to restore the shape of the defect area; (C) virtual restoration of the maxillary defect with an iliac crest flap; (D) 3D-printed craniomaxillary model and pre-bent titanium plate.

Step 5 was the intraoral anastomosis. The vascular pedicle was transferred to the recipient area on the buccal mucosa. An end-to-end arterial anastomosis was made between the DCIA and the facial artery or the superior labial artery. The venous anastomosis was made between the deep circumflex iliac vein and the facial vein in the same way (Fig. 4B). Good inflow and outflow of blood and satisfactory perfusion of the flap were confirmed.

Step 6 – reconstruction of the orbital floor – was performed in the case of a Brown class III maxillary defect. Using the mirroring technique, the shape of the defective orbital floor was restored in ProPlan CMF 3.0, and a 3D model was printed. During surgery, pre-bent

titanium mesh, moulded according to the shape of the 3D-printed craniomaxillary model, was placed and fixed to the remnant peri-orbital structures with titanium screws (Fig. 5).

#### Follow-up

Postoperative complications at the donor site (e.g., pain, gait disturbances, hernia) and the recipient site (e.g., flap failure, infection, iatrogenic facial nerve injury) were recorded. The patients were asked to self-evaluate their satisfaction with their postoperative appearance.

Spiral CT of the maxillofacial region was repeated at 1 week after surgery. As before, 3D reconstruction was performed, and the craniomaxillary model was

imported in STL format into Geomagic Control 2014 (3D Systems) for comparison with the craniomaxillary model obtained preoperatively. The non-surgical areas of the two models were used to achieve correct alignment. The accuracy of the surgical reconstruction was evaluated by colour map analysis (Fig. 6).

Using ProPlan CMF 3.0, a mirror skull was generated with the mirror technique. The midsagittal plane was defined using the anterior nasal spine, nasion point, and midpoint of the posterior border of foramen magnum. The head position was adjusted with the Frankfort plane as the horizontal plane. From the bottom view of the defect area, the horizontal relationship between the mirror dentition and iliac block could be clearly judged

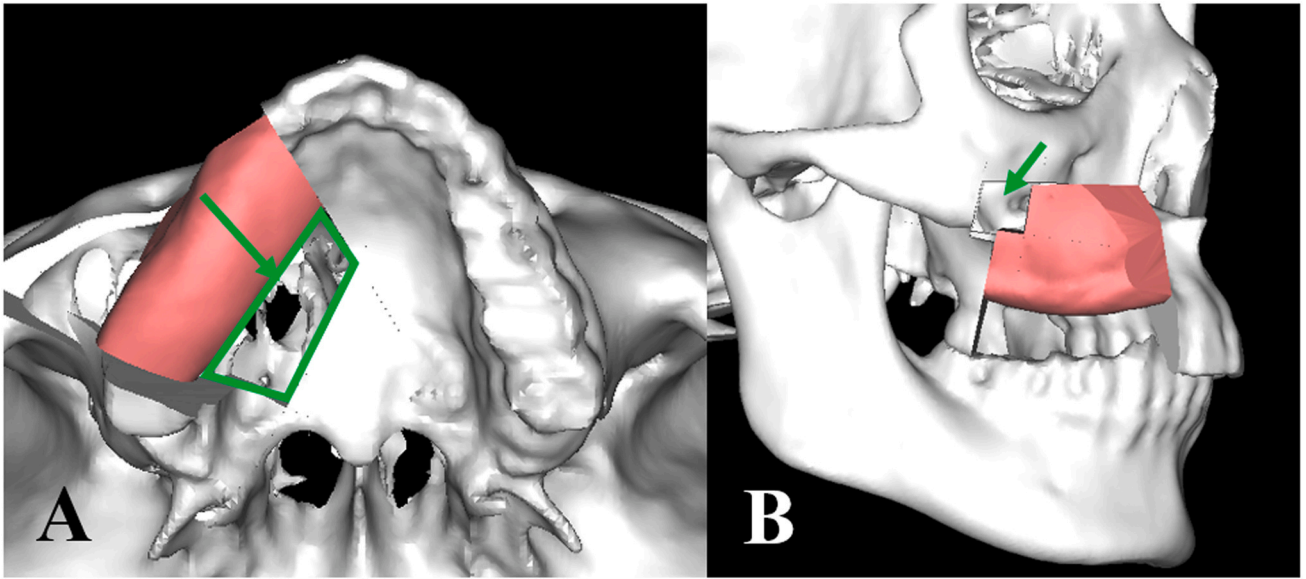


Fig. 2. Consideration of the vascular pedicle of the DCIA flap: (A) an area where part of the hard palate was resected for the safety of flap vessels; (B) a passage created at the posterior border of the defect area for the flap vessels.

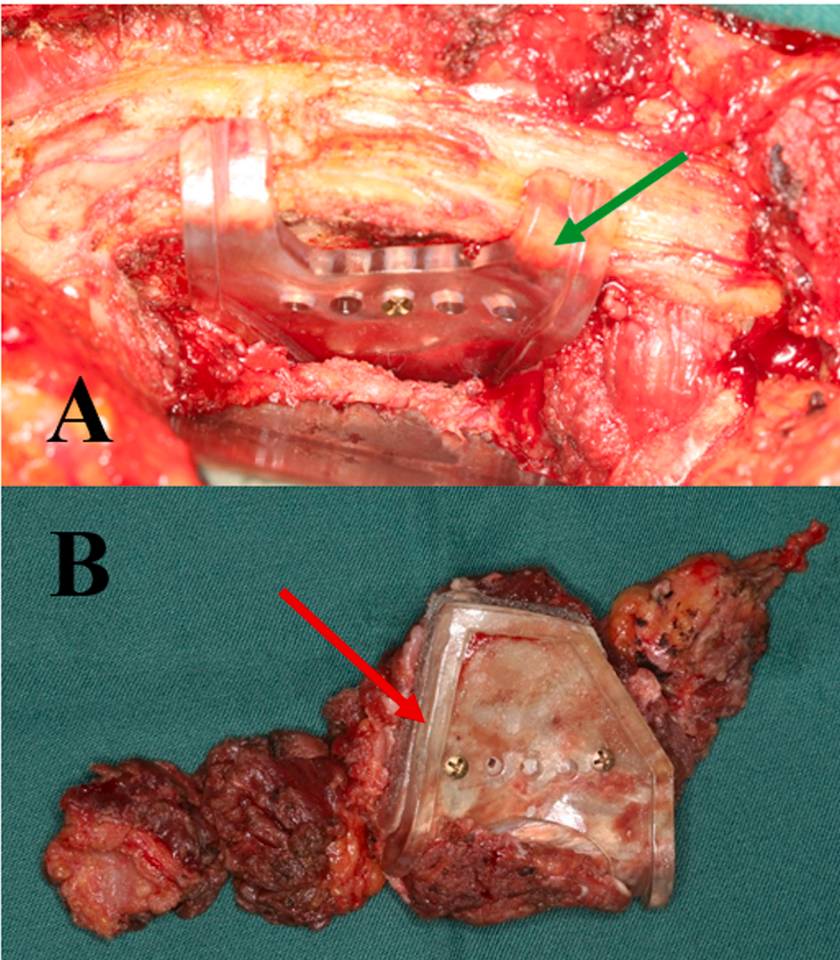


Fig. 3. Harvesting of the DCIA flap: (A) placement and fixation of the iliac osteotomy guide; (B) DCIA flap preparation guided by the iliac osteotomy guide.

(Fig. 7). For a tooth in the mirror dentition, if more than half of it was located on the iliac block, it was considered a suitable site for implant placement. The implant site coverage rate was defined as the number of mirror teeth with a suitable site for implant placement as a percentage of the number of missing teeth in the defect area.

**Results**

The median age of the 11 patients (six female and five male) was 34 years (age range 15–55 years). Intraoral anastomosis was successful in nine patients (patients 1–5, 7–10). For two of these nine patients (patients 9, 10), the anastomosed arteries were twisted after flap positioning and fixation, and so re-anastomosis was needed. The nine patients with successful intraoral anastomosis had good aesthetic outcomes. The recipient arteries for intraoral anastomosis were the facial artery (seven patients) and superior labial artery (two patients); the recipient vein was the facial vein (all nine patients). Intraoral anastomosis failed in one patient (patient 6), because the calibre of the recipient vessels was small. As a result, the blood supply to the flap was poor after intraoral anastomosis. In this case, submandibular extraoral anastomosis was adopted as an alternative and was successful.

The flap survived, with no major complications, in 10 of the 11 patients in this series (patients 1–10). However, the DCIA flap failed in one patient (patient

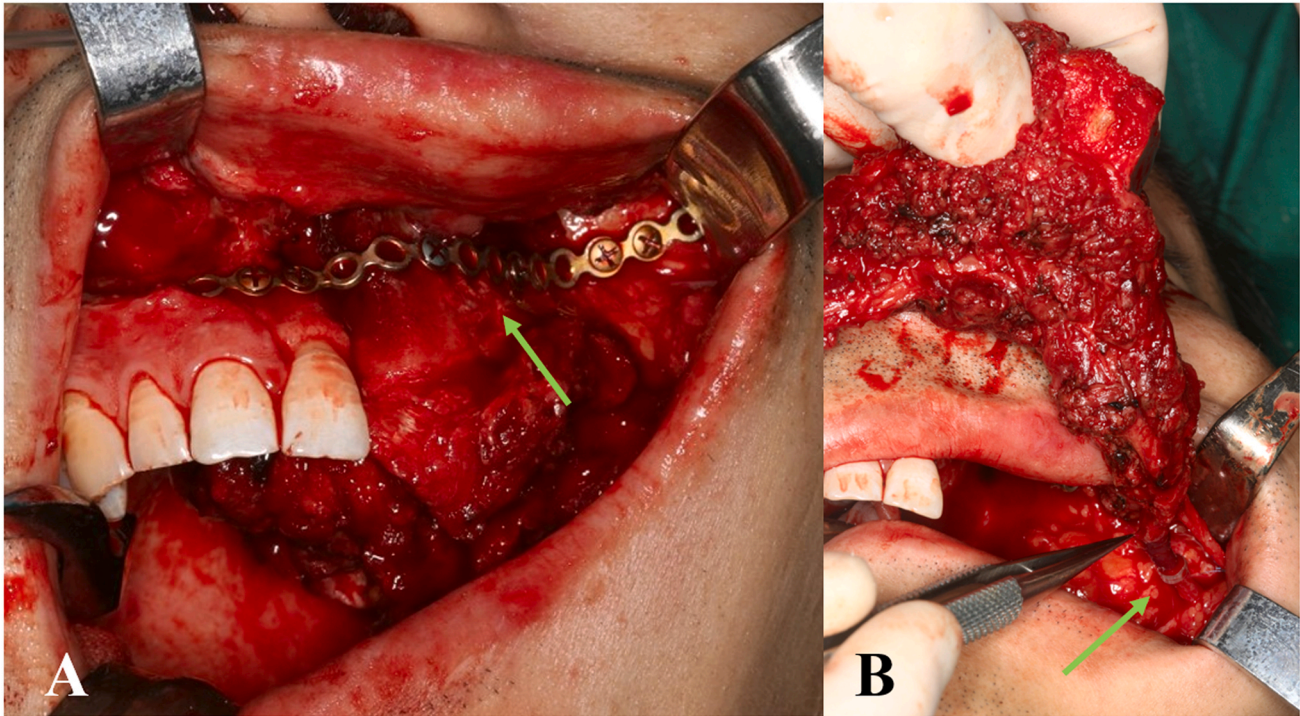


Fig. 4. Surgical implementation: (A) placement and fixation of the DCIA flap; (B) intraoral anastomosis.

11) due to recipient vein thrombosis 1 day after the operation, and it had to be removed. The Brown classification of the defect varied among the 10 patients with successful DCIA flap transplantation (patients 1–10); the vertical classifications included classes I, II, and III, and the horizontal classifications included classes b, c, and d (Table 1). An ideal bone height was achieved in all 10 patients, with the crest of the DCIA flap reaching

the same height as the remnant alveolar ridge (Fig. 8). No serious donor site complications occurred in any patient. Table 2 presents more details of the DCIA flaps.

Among the 10 patients in whom the flap survived, colour map analysis showed a mean deviation of  $0.40 \pm 0.08$  mm between the preoperative and postoperative craniomaxillary models. The deviation was  $\leq 1$  mm in  $92.70\% \pm 2.26\%$  of the

regions,  $\leq 2$  mm in  $95.68\% \pm 1.44\%$  of regions, and  $\leq 3$  mm in  $97.17\% \pm 1.04\%$  of regions. All 10 patients were satisfied with their postoperative appearance.

The implant site coverage rate results are presented in Table 3. The mean implant coverage rate was 89.46%.

All three patients with a Brown class III maxillary defect and orbital floor reconstruction had good outcomes, with no serious complications (visual impairment, eye movement disorder, or titanium mesh exposure).<sup>10</sup>

After maxillary reconstruction, seven patients also underwent dental implantation (Fig. 9). A total of 19 implants were placed. The interval between maxillary reconstruction and dental implantation was 7–11 months (mean 9 months). All implants achieved good primary stability, and all seven patients were satisfied with their functional outcomes after dental implantation. No implants have been lost to date (after a mean follow-up of 10 months); thus, the implant survival rate is 100%.

Four patients have not as yet undergone dental implantation. Among them, one patient could not receive dental implants because of flap failure and removal (patient 11). One patient has not been able to undergo dental implantation temporarily because of a postoperative infection



Fig. 5. Titanium mesh moulded on the 3D-printed craniomaxillary model.

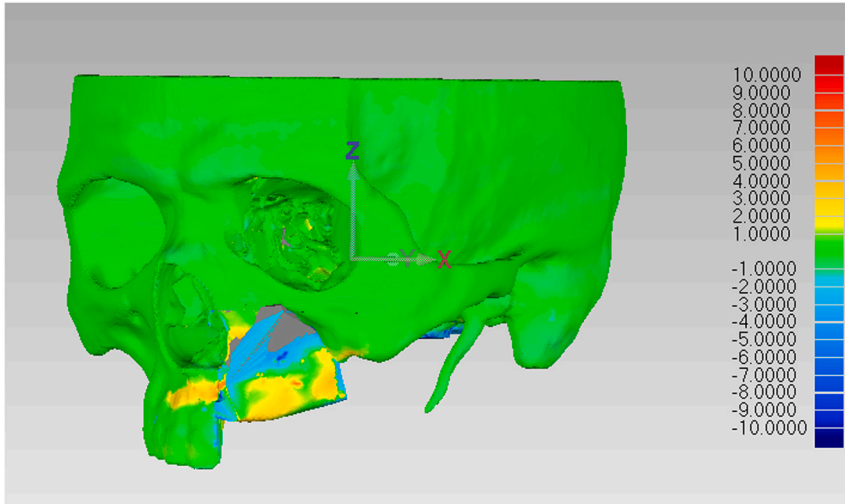


Fig. 6. Postoperative 3D colour map analysis.

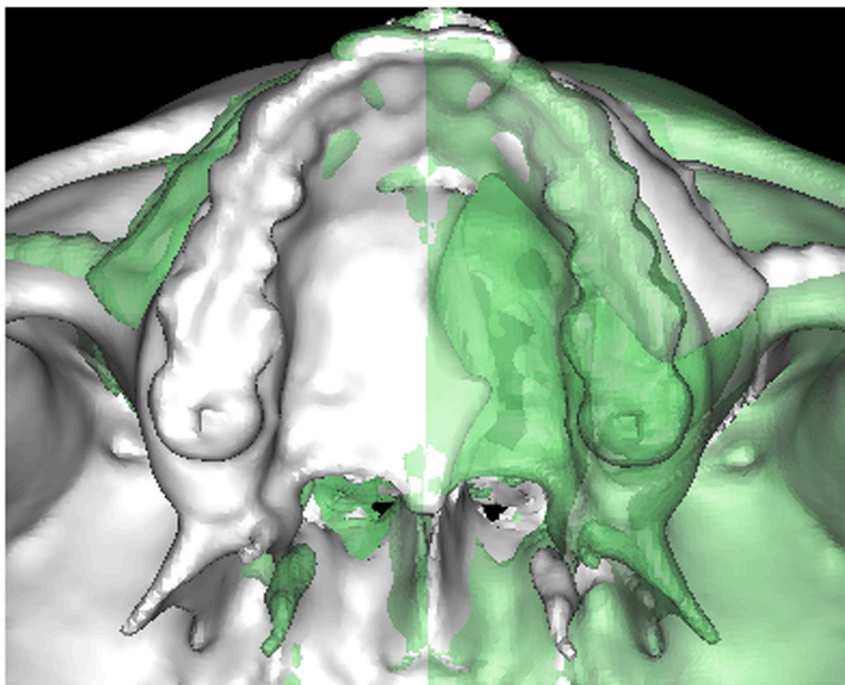


Fig. 7. Evaluation of the implant site coverage rate.

(patient 7). The titanium plate has been removed and debridement has been performed. The patient is still under recovery and follow-up. Two patients have refused to accept dental implantation for financial reasons (patients 4, 8).

Regarding the aesthetic outcomes, an extraoral incision was avoided in eight patients (patients 1–3, 5, 7–9, 11). The tumour was exposed through the incision at the vestibular groove and palate. However, extraoral incisions were performed in three patients (patients 4, 6, 10). For patient 6, a submandibular

incision was performed for extraoral anastomosis because of the failure of intraoral anastomosis. For patients 4 and 10, a Weber–Ferguson incision was performed because the tumour affected the orbital floor. Part of the orbital floor needed to be resected.

### Discussion

Although the DCIA flap is considered the gold standard for maxillary reconstruction,<sup>3,4,11</sup> a major shortcoming is its short vascular pedicle of only about 5 cm.<sup>1,5,6,12</sup>

In the series of patients presented here, an intraoral anastomosis was used to overcome this problem<sup>13–16</sup> and was successful in nine of the 11 patients.

Intraoral anastomosis was first reported by Gaggl et al. in 2009.<sup>13</sup> With this technique, facial scars can be avoided and the required length of the vascular pedicle can be reduced. Other researchers have since carried out similar studies on intraoral anastomosis and have achieved good results.<sup>1,5,6,15,16</sup> However, in the present study, intraoral anastomosis posed problems in four patients (patients 6, 9–11), all of whom had defects located in the posterior maxilla and extending beyond the maxillary first molar. It is speculated that this may be one of the reasons for the problems with intraoral anastomosis. The recipient vessels in intraoral anastomosis are usually the facial artery and facial vein, which are located approximately in the buccal mucosa area of the maxillary first molar.<sup>12</sup> Meanwhile, the vessels of the DCIA flap are usually placed distally. When the defect does not extend beyond the maxillary first molar, the vessels of the DCIA flap can travel directly to the recipient vessel area without bending. However, when the defect extends beyond the maxillary first molar, the vessels of the DCIA flap need to be turned to the mesial side by 180° to reach the recipient vessel. It is believed that this 180° turning contributes to the failure of intraoral anastomosis, both by increasing the risk of thrombosis and by increasing tension in the vessel wall. Regarding the defect size, the present authors do not consider this a factor affecting the success rate of intraoral anastomosis in DCIA reconstruction of the maxilla. The number of missing teeth in the defect area can reflect the defect size. For the four patients with problems in intraoral anastomosis, the number of missing teeth in the defect area ranged from 3 to 7, with a mean of 4.75. This is not significantly different from the overall mean defect size.

Apart from the location of the defect, the pathological type of disease also has an impact on the application of the reported technique. It is more suitable for patients with benign disease than for those with malignant disease, mainly because the extent of malignant lesions cannot be determined accurately preoperatively. The area of resection often needs to be adjusted intraoperatively according to the results of intraoperative biopsy margin

Table 1. Patient characteristics.

Patient	Sex	Age (years)	Diagnosis	Brown classification of defect
1	Male	23	Ossifying fibroma	IId
2	Male	33	Maxillary defect secondary to trauma 6 months ago	IIId
3	Male	31	Ossifying fibroma	I Ib
4	Male	36	Ossifying fibroma	IIIb
5	Female	34	Odontogenic myxoma	I Ib
6	Female	35	Maxillary defect secondary to maxillectomy for mucoepidermoid carcinoma 17 years ago	I Ib
7	Female	38	Ossifying fibroma	I b
8	Male	37	Epithelial verrucous carcinoma	I Ic
9	Female	28	Calcifying epithelial odontogenic tumour	I b
10	Female	15	Ossifying fibroma	IIIb
11	Female	55	Moderately differentiated carcinoma	I Ib
Mean age		33		

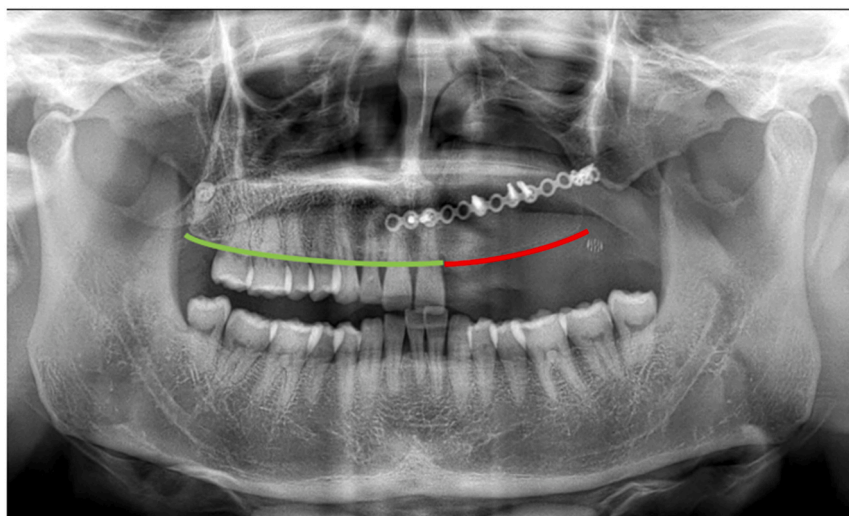


Fig. 8. Panoramic radiograph of the patient shown in Figs. 1 and 2. The green line outlines the alveolar ridge of the residual maxilla and the red line outlines the iliac crest of the flap.

analysis. Thus, accurate preoperative design of both the resection and reconstruction is not generally possible.

Nowadays, increasing attention is being paid to the occlusal reconstruction following the bone reconstruction.<sup>17</sup> In this study, virtual surgery planning was performed under the guidance of an occlusion-driven reconstruction concept. Focus was placed on restoring the position and structure of the alveolar process according to the need for subsequent restoration of the dentition. Furthermore, the DCIA flap was placed with the iliac crest facing downward, as the cortex of the iliac crest can provide better primary stability for the implant. Moreover, the wider width of iliac crest compared with the non-iliac crest side can provide more flexibility for implant site selection.

The normal maxilla has three buttress structures: the nasomaxillary buttress, zygomaticomaxillary buttress, and pterygomaxillary buttress.<sup>18</sup> These buttress structures provide mechanical support for maxillary mastication

Table 2. Iliac flap characteristics.

Patient	Iliac segment	Iliac length (cm)	Iliac height (cm)	Length of preserved ASIS (cm)	Recipient artery	Recipient vessel
1	2	6.3 (3.3 + 3)	2.2	2	Facial artery	Facial vein
2	2	6.2 (3.6 + 2.6)	3	2	Facial artery	Facial vein
3	1	4.5	3	6.4	Facial artery	Facial vein
4	2	7.2 (3.5 + 3.7)	2.3	0	Facial artery	Facial vein
5	1	5.5	4	0	Facial artery	Facial vein
6	1	2.6	2.3	1	Facial artery	Branch of jugular vein
7	1	3.2	2.5	2.3	Superior labial artery	Facial vein
8	1	6.5	2.6	2.8	Facial artery	Facial vein
9	1	3.8	2.2	2	Facial artery	Facial vein
10	2	5.5 (3 + 2.5)	2.6	2.4	Superior labial artery	Facial vein
11	1	4.7	2.5	2	Facial artery	Facial vein
Mean ± SD		5.1 ± 1.5	2.7 ± 0.5			

ASIS, anterior superior iliac spine; SD, standard deviation

Table 3. Patient implant site coverage rate.

Patient	Number of missing teeth in defect area	Number of teeth with suitable site for implant	Implant site coverage rate (%)
1	8	7	87.5
2	8	7	87.5
3	5	4	80
4	6	5	83.3
5	4	4	100
6	4	4	100
7	3	3	100
8	8	8	100
9	4	4	100
10	5	3	60
11	7	6	85.7
Mean	5.64	5	89.46

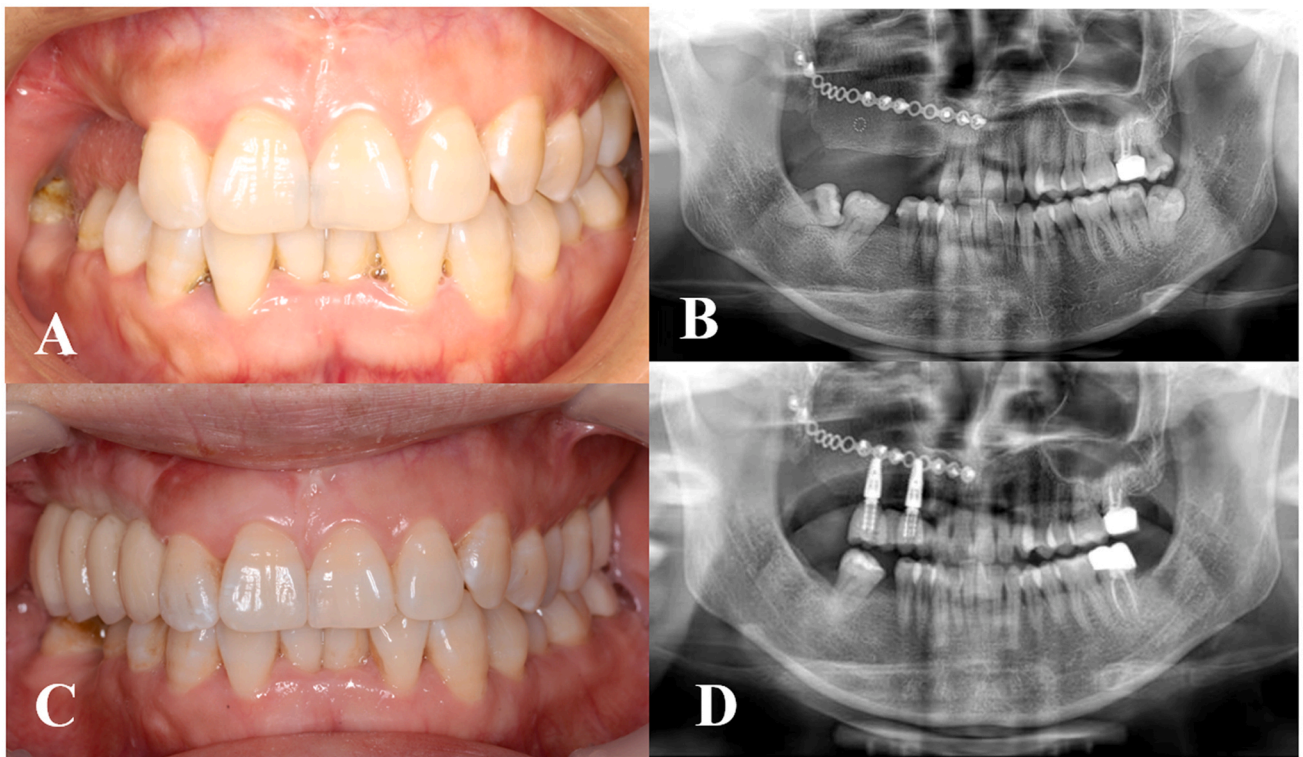


Fig. 9. Postoperative images: (A) intraoral photograph and (B) panoramic radiograph obtained at 9 months after surgery before dental rehabilitation; (C) intraoral photograph and (D) panoramic radiograph obtained after dental rehabilitation.

function. To ensure support for future implants and prostheses, the buttress structures must be restored during maxillary reconstruction. The iliac crest can provide sufficient bone volume to achieve this goal. Previous researchers have shown that the DCIA flap can be shaped according to the four processes of the normal maxilla so that the iliac block can contact the surrounding bone. By doing so, all three buttress structures can be restored. However, the iliac block will deviate from the position of the alveolar process, which is not conducive to subsequent implant restoration.<sup>3</sup> Therefore, in the patients

presented in this case series, focus was first placed on restoring the position and structure of the alveolar process. On this basis, at least one of the three buttress structures was restored to make sure that the DCIA flap would provide adequate support for implants and prostheses.

Due to the complex morphology of the maxilla, reconstruction with the DCIA flap can be difficult.<sup>15</sup> Performing intraoral anastomosis in the limited surgical space only adds to the difficulty of the operation. Further, there is the need to consider restoration of the alveolar process and buttress structures.

CAD/CAM technology can be very helpful in addressing these challenges. In this study, a computer-assisted navigation system was used to guide the tumour resection and verify the position of the iliac block.<sup>19</sup> The use of individualized 3D-printed iliac osteotomy guides and pre-bent titanium plates decreased the operation time and ensured accurate positioning of the iliac block.<sup>20</sup> Osteotomy and placement guides were not used, as they cannot be placed in the mouth without adopting the Weber-Ferguson approach. Overall, the application of CAD/CAM decreased the operation time, reduced the difficulty of

the operation, and achieved greater accuracy than with other methods.<sup>1,5,21,22</sup>

In summary, the findings of this study indicate that occlusion-driven maxillary reconstruction with a DCIA flap using CAD/CAM and intraoral anastomosis techniques is feasible and accurate. The use of CAD/CAM technology delivered good accuracy. The proposition and practice of our understanding on occlusion-driven reconstruction brought good functional outcomes for patients. Besides, we discussed the indications and limitation of intraoral anastomosis for DCIA reconstruction of maxilla. For posterior maxillary defects, this method may be associated with some risk, hence there should be careful patient selection. The sample size of this study was small and the follow-up time was short, therefore the conclusions should be interpreted with caution.

### Ethical approval

This study was approved by the Ethics Committee of Peking University School of Stomatology (approval number PKUSSIRB202055065).

### Funding

This work was supported by the Capital Funds for Health Improvement and Research (2020–2–4102) and National Program for Multidisciplinary Cooperative Treatment on Major Diseases (PKUSSNMP-202015).

### Patient consent

All patients involved in this study signed the informed consent to use their clinical data and images.

### Competing interests

None.

### References

- Jie B, Lv X, Zheng L, Zhang Y, He Y. New series of surgical design for anterior maxillary reconstruction with deep circumflex iliac artery flap. *Head Neck* 2020; **42**:3438–45.
- Kang YF, Liang J, He Z, Xie S, Zhang L, Shan XF, Cai ZG. Cortical bone resorption of fibular bone after maxillary reconstruction with a vascularized fibula free flap: a computed tomography imaging study. *Int J Oral Maxillofac Surg* 2019; **48**:1009–14.
- Brown JS, Shaw RJ. Reconstruction of the maxilla and midface: introducing a new classification. *Lancet Oncol* 2010; **11**:1001–8.
- Brown JS. Deep circumflex iliac artery free flap with internal oblique muscle as a new method of immediate reconstruction of maxillectomy defect. *Head Neck* 1996; **18**:412–21.
- Zheng L, Lv X, Shi Y, Zhang J, Zhang J. Intraoral anastomosis of a vascularized iliac-crest flap in maxillofacial reconstruction. *J Plast Reconstr Aesthet Surg* 2019; **72**:744–50.
- Zheng L, Wu W, Shi Y, Zhang J. Mandibular reconstruction with a deep circumflex iliac artery flap using computer-assisted and intraoral anastomosis techniques. *J Oral Maxillofac Surg* 2019; **77**:2567–72.
- Wang F, Bornstein MM, Hung K, Fan S, Chen X, Huang W, Wu Y. Application of real-time surgical navigation for zygomatic implant insertion in patients with severely atrophic maxilla. *J Oral Maxillofac Surg* 2018; **76**:80–7.
- Gerbino G, Zavattero E, Berrone M, Berrone S. Management of needle breakage using intraoperative navigation following inferior alveolar nerve block. *J Oral Maxillofac Surg* 2013; **71**:1819–24.
- Bettschart C, Kruse A, Matthews F, Zemann W, Obwegeser JA, Gratz KW, Lubbers HT. Point-to-point registration with mandibulo-maxillary splint in open and closed jaw position. Evaluation of registration accuracy for computer-aided surgery of the mandible. *J Craniomaxillofac Surg* 2012; **40**:592–8.
- Kang YF, Liang J, He Z, Zhang L, Shan XF, Cai ZG. Orbital floor symmetry after maxillectomy and orbital floor reconstruction with individual titanium mesh using computer-assisted navigation. *J Plast Reconstr Aesthet Surg* 2020; **73**:337–43.
- Politi M, Toro C. Iliac flap versus fibula flap in mandibular reconstruction. *J Craniofac Surg* 2012; **23**:774–9.
- Peng X, Mao C, Yu GY, Guo CB, Huang MX, Zhang Y. Maxillary reconstruction with the free fibula flap. *Plast Reconstr Surg* 2005; **115**:1562–9.
- Gaggl A, Burger H, Virnik SA, Chiari FM. An intraoral anastomosing technique for microvascular bone flaps in alveolar ridge reconstruction: first clinical results. *Int J Oral Maxillofac Surg* 2009; **38**:921–7.
- Stalder MW, Sosin M, Urbinelli LJ, Mayo JL, Dorafshar AH, Hilaire HS, Borsuk DE, Rodriguez ED. Avoiding facial incisions with midface free tissue transfer. *Plast Reconstr Surg Glob Open* 2017; **5**:e1218.
- Brandtner C, Burger H, Hachleitner J, Gaggl A. The intraoral anastomosing technique in reconstructive surgery of the face—a consecutive case series of 70 patients. *J Craniomaxillofac Surg* 2015; **43**:1763–8.
- Sosin M, Sinada GG, Rodriguez ED, Dorafshar AH. Intraoral microvascular anastomosis of an iliac free flap for maxillary fibrous dysplasia. *J Oral Maxillofac Surg* 2015; **73**:e2061–5.
- Zhang M, Rao P, Xia D, Sun L, Cai X, Xiao J. Functional reconstruction of mandibular segment defects with individual preformed reconstruction plate and computed tomographic angiography-aided iliac crest flap. *J Oral Maxillofac Surg* 2019; **77**:1293–304.
- Medeiros YL, Loures AO, Silva BN, Reher P, Devito KL, Carvalho MF. Tomographic analysis of nasomaxillary and zygomatico-maxillary buttress bone thickness for the fixation of miniplates. *Int J Oral Maxillofac Surg* 2021; **50**:1034–9.
- Shan XF, Chen HM, Liang J, Huang JW, Cai ZG, Guo CB. Surgical navigation-assisted mandibular reconstruction with fibula flaps. *Int J Oral Maxillofac Surg* 2016; **45**:448–53.
- Qiu S, Kang Y, Ding M, Zhang Y, Zhu HW, Zhang L, Shan XF, Cai ZG. Mandibular reconstruction with the iliac flap under the guidance of a series of digital surgical guides. *J Craniofac Surg* 2021; **32**:1777–9.
- Chang EI, Boukvalas S, Liu J, Largo RD, Hanasono MM, Garvey PB. Reconstruction of posterior mandibulectomy defects in the modern era of virtual planning and three-dimensional modeling. *Plast Reconstr Surg* 2019; **144**:453e–62e.
- Mazzola F, Smithers F, Cheng K, Mukherjee P, Low TH, Ch'ng S, Palme GE, Clark JR. Time and cost-analysis of virtual surgical planning for head and neck reconstruction: a matched pair analysis. *Oral Oncol* 2020; **100**:104491.

Correspondence to: Department of Oral and Maxillofacial Surgery  
Peking University School and Hospital of Stomatology  
22 Zhongguancun South Avenue  
Haidian District  
100081 Beijing  
China.  
E-mail: c2013xs@163.com